Journal of Sound and Vibration (2000) **230**(2), 393–410
doi:10.1006/jsvi.1999.2606, available online at http://www.idealibrary.com on IDEAL®

AN EFFICIENT METHOD FOR CALCULATING R.M.S. VON MISES STRESS IN A RANDOM VIBRATION ENVIRONMENT †

DANIEL J. SEGALMAN, CLAY W. G. FULCHER, GARTH M. REESE, AND RICHARD V. FIELD JR

Structural Dynamics and Vibration Control Department, Sandia National Laboratories, P.O. Box 5800, *Mail stop* 0847, *Albuquerque, NM* 87185-0847, *U.S.A.*

(*Received* 14 *September* 1998, *and in final form* 3 *September* 1999)

A rigorous and efficient method is presented for calculation of root-mean-square (r.m.s.) von Mises stresses for linear structures excited by stationary random loads. The r.m.s. value is expressed in terms of the zero time-lag covariance matrix of the loads, which in most applications of structural analysis will be calculated from frequency-domain, stress-component transfer functions and the cross-spectral density matrix of the applied loads. The key relation presented is one suggested in past literature, but that does not appear to have been exploited previously in this manner. The exact determination of r.m.s. von Mises stress is used to demonstrate that the Miles relation, commonly used in design, can be conservative or non-conservative. Finally, because of the efficiency with which the exact r.m.s. von Mises stress can be calculated, the analyst can now perform surveys on von Mises stresses routinely, allowing a thorough investigation into the reliability of an engineering design.

© 2000 Academic Press

1. INTRODUCTION

Increasingly, computational methods—especially finite element techniques—are expected to *predict* the reliability of components and systems. This trend is driven both by the advancing variety and capabilities of the numerical tools available, and by a decreasing tolerance for the cost of exhaustive testing. In this monograph, the issue of predicting reliability of structures subject to a class of random loadings is examined where failure is associated with values of von Mises stress near yield. This problem is substantially more difficult than that of deterministic problems of statics and dynamics, since the input forces are known only statistically and the responses must also be statistical in nature. Further, because von Mises stress is a non-linear function of the stress components, methods of the theory of random vibration

† This paper was presented at the 16th International Modal Analysis Conference, sponsored by the Society for Experimental Mechanics, Bethel, Connecticut, www.sem.org.

0022-460X/00/070393 + 18 $35.00/0 © 2000 Academic Press

normally applied to compute the statistics of acceleration, displacement, or stress components responses cannot be applied directly to calculate the von Mises stress. A thorough discussion of the non-deterministic response of linear systems can be found in reference [1] and a discussion more in the context of these problems can be found in references [2, 3].

The most direct method of calculating von Mises stress from frequency data requires computation of a long time series of linear stress components. The stress invariants can be computed at each time step and an root-mean-square (r.m.s.) value determined through time integration. The expense of this computational procedure makes its use in broad surveying for von Mises stress impractical. Computationally simpler methods, such as Miles' relation [4], involve significant approximations that can be non-conservative [5].

What is ultimately sought is the probability distribution of von Mises stress in terms of the statistical properties of the applied forces. In this monograph, it is shown how part of the leap from the statistics of the input forces to the probability distribution of the von Mises stress is achieved. Specifically, an explicit expression for the r.m.s. values of von Mises stress, computed directly from frequency domain terms is given. This new method enables the analyst to perform surveys of von Mises stress routinely, allowing a thorough investigation into the reliability of an engineering design, while accounting for the full frequency response of the structure.

2. THE PROBLEM

In a typical random vibration test, a structure is attached to a single-input load source, such as a shaker table, and subjected to a vibratory load characterized by a specified power spectral density (PSD) of the input acceleration. Accelerometers and strain gages distributed over the test object can be used to verify the fidelity of finite element modal analysis. The problem faced by a structural analyst is then to assess whether the stress fields generated in the structure approach failure. For ductile materials, it is von Mises stress that provides that metric, and the analyst needs a tool mapping the statistics of the input force to some statistical measure of the resulting von Mises stress.

To illustrate the problem, a finite element model of an aluminium cylinder, subjected to transverse random vibration at the base, was created using shell elements. Figures 1 and 2 show the cylinder model and the input acceleration PSD applied at the base, respectively.

Current standard procedure is to choose a single modal frequency (typically the one associated with highest modal effective mass [6] within the bandwidth of the input) and to use the modal damping and the PSD of the input acceleration at that frequency in Miles' relation to compute an "equivalent static g-field". A static stress analysis is performed as though the structure were subject to a gravity load at that g level. Response contributions from other structural frequencies are ignored and no use is made of any mode shape. If this selected mode dominates all others and if it resembles the static deformation, this method can result in a reasonable estimate

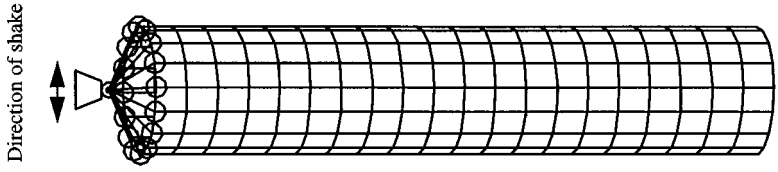

Figure 1. Finite element model of cylinder.

of the stress distribution. Very often this method is inaccurate for ascertaining the global random stress response.

A method is derived here that accurately and efficiently captures the contributions to r.m.s. von Mises stress from all excited modes throughout the structure, and for all frequencies of interest.

3. R.M.S. VON MISES STRESS

The von Mises stress, $p(t)$, is a scalar defined so that its square is a quadratic function of stress:

$$p(t)^2 = \sigma(t)^{\mathrm{T}} A \sigma(t), \tag{1}$$

where $\sigma = [\sigma_{xx}\, \sigma_{yy}\, \sigma_{zz}\, \sigma_{yz}\, \sigma_{xz}\, \sigma_{xy}]^{\mathrm{T}}$ is the stress "vector" of non-redundant components of the stress tensor [7], and

$$A = \begin{bmatrix} 1 & -\frac{1}{2} & -\frac{1}{2} & & & \\ -\frac{1}{2} & 1 & -\frac{1}{2} & & & \\ -\frac{1}{2} & -\frac{1}{2} & 1 & & & \\ & & & 3 & & \\ & & & & 3 & \\ & & & & & 3 \end{bmatrix}. \tag{2}$$

Expressing the stress in terms of modal co-ordinates,

$$\sigma(t) = \sum_k q_k(t)\, \Psi_k^{\sigma}, \tag{3}$$

where Ψ_k^{σ} is a column vector of the stress components (1–6) for mode k at the location of interest, and $q_k(t)$ is the kth modal co-ordinate at that time. Summation

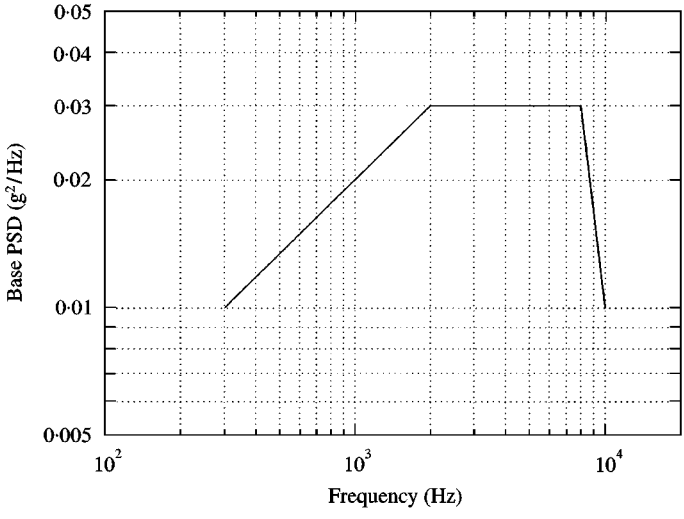

Figure 2. Input transverse PSD at cylinder base.

in the above equation is over all modes. Substituting equation (3) into equation (1), we express the square of von Mises stress in terms of modal co-ordinates:

$$p^2(t) = \sum_i \sum_j q_i(t) q_j(t) \Psi_i^{\sigma \mathrm{T}} A \Psi_j^{\sigma} . \tag{4}$$

This expression for von Mises stress in terms of modal co-ordinates is new.

Taking expected values of both sides of equation (4) and exploiting the linearity of this operator, we obtain the following expression for the mean-square value of von Mises stress:

$$E[p^2(t)] = \sum_{i,j} \Gamma_{ij} T_{ij}, \tag{5}$$

where

$$T_{ij} = \Psi_i^{\sigma \mathrm{T}} A \Psi_j^{\sigma} \tag{6}$$

and

$$\Gamma_{ij} = E[q_i(t) q_j(t)] \tag{7}$$

is the zero time-lag cross-covariance between the ith and jth modal co-ordinates. Note that the matrix Γ is a modal quantity whereas T varies spatially over the structure. The above expression (5) for the mean-square of von Mises stress is also new.

The mathematics used to evaluate Γ in terms of the input forces is conventional, but its implementation in the context of this application of structural analysis deserves discussion.

Equation (5) applies to the stationary response of any linear structure. To exploit the tools that are readily available to the structural dynamicist, numerical

evaluation of mean-square von Mises stress is facilitated by Fourier methods that are restricted to problems of loads of zero mean. For simplicity, the rest of this development will assume that all loads are of zero mean. Problems where the loads are stationary but not of zero mean are accommodated by a small extension presented in Appendix A.

The Fourier transforms of the modal co-ordinates are expressed in terms of the Fourier transforms of the input forces via appropriate frequency response functions of the system [8, p. 506]:

$$\hat{q}_i(\omega) = H_{ij}(\omega)\hat{f}_j(\omega), \tag{8}$$

where the column vector $\hat{q}(\omega)$ is the Fourier transform of q, $\hat{f}(\omega)$ is the Fourier transform of f, and $H(\omega)$ is the matrix of transfer functions between them. Standard manipulations [8, pp. 506–508] yield the cross-spectral density matrix for the q in terms of the cross-spectral density matrix for the applied loads:

$$S_{qq}(\omega) = \overline{H(\omega)}\, S_{ff}(\omega) H(\omega)^{\mathrm{T}}, \tag{9}$$

where

$$S_{qq}(\omega)_{ij} = \int_{-\infty}^{\infty} R_{q_i q_j}(\tau) \mathrm{e}^{-\mathrm{i}\omega\tau}\, \mathrm{d}\tau \quad \text{and} \quad S_{ff}(\omega)_{ij} = \int_{-\infty}^{\infty} R_{f_i f_j}(\tau) \mathrm{e}^{-\mathrm{i}\omega\tau}\, \mathrm{d}\tau, \; R_{xy}(\tau)$$

is the matrix of covariances of the Cartesian product of column vectors x and y, and $\overline{(\,)}$ is the complex conjugate. The cross-spectral density matrix of applied loads, $S_{ff}(\omega)$, is often the form in which applied loads are specified to the analyst.

From Plancherel's theorem [9, pp. 187–189], we have the well-known expression for covariance in terms of spectral density [10, p. 123]:

$$\Gamma = \frac{1}{2\pi}\int_{-\infty}^{\infty} S_{qq}(\omega)\, \mathrm{d}\omega = \frac{1}{2\pi}\int_{-\infty}^{\infty} \overline{H(\omega)}\, S_{ff}(\omega) H(\omega)^{\mathrm{T}}\, \mathrm{d}\omega. \tag{10}$$

Equations (5), (6), and (10) provide an explicit expression for the mean square of von Mises stress. The one-dimensional version of this expression has been used previously in stress analysis [5, 11], but the equations presented here appear to be the first that accommodate the full stress tensor, and thus can be incorporated into structural analysis.

Another interesting expression can be obtained by substituting equations (10) and (6) into equation (5) and rearranging the terms:

$$E[p^2(t)] = \sum_m \sum_n \frac{1}{2\pi}\int_{-\infty}^{\infty} [(H^{\sigma}(\omega))^{\dagger} A H^{\sigma}(\omega)]_{mn}\, S_{ff}(\omega)_{mn}\, \mathrm{d}\omega, \tag{11}$$

where $H^{\sigma}_{ra}(\omega) = \sum_k \Psi^{\sigma}_{kr} H_{ka}(\omega)$ is the frequency response function of the rth stress component due to the ath force and $(\,)^{\dagger}$ is the Hermitian operator. Equation (11) is

particularly interesting because it expresses the mean-square von Mises stress as an integral over frequency, without any direct reference to vibrational modes.

4. COMPUTATION OF R.M.S. VON MISES STRESS IN STRUCTURAL ANALYSIS

The components that combine to form equation (5) are natural elements of modern structural analysis. The modal frequencies, mode shapes, and even the modal stress responses, $\Psi^b_{\sigma,i}$ are standard output from most FEA modal analysis codes (such as the grid point stress in MSC/NASTRAN [12]). Modal damping, and damping generally in structural dynamics, is usually assigned in an *a posteriori* manner.

For a modally damped structure, the modal transfer function for modal co-ordinate k due to an input force at degree of freedom a, can be written as [13]

$$H_{ka}(\omega) = \frac{\varphi_{ak}}{\omega_k^2 - \omega^2 + 2j\gamma_k\omega_k\omega} = \varphi_{ak} D_k(\omega). \tag{12}$$

Here, φ_{ak} is the ath component of the kth displacement eigenvector, ω_k is the kth modal frequency, and γ_k is the kth modal damping. Note that D contains all frequency dependence. The zero time-lag covariance matrix is obtained by substituting equation (12) into equation (10):

$$\Gamma_{ij} = \sum_a^{N_F}\sum_b^{N_F} \phi_{ai}\phi_{bj}\left(\frac{1}{\pi}\int_0^\infty \mathrm{Re}(\overline{D_i(\omega)} D_j(\omega)[S_{ff}(\omega)]_{ab})\,\mathrm{d}\omega\right), \tag{13}$$

where use has been made of the fact that each of the factors in the above integral is the Fourier transform of a real function.

In application, the integral is approximated by a summation over discrete, evenly spaced frequencies:

$$\Gamma_{ij} = \sum_a^{N_F}\sum_b^{N_F} \phi_{ai}\phi_{bj}\sum_{n=1}^{N_\omega} \mathrm{Re}(\overline{D_i(\omega_n)} D_j(\omega_n)[S_{ff}(\omega_n)]_{ab})\frac{\Delta\omega}{\pi}. \tag{14}$$

The discrete summation is natural for these problems since the cross-spectral density matrix of forces can be obtained via fast Fourier transforms of digitized experimental data.

For a single shaker input, $N_F = 1$, and equation (14) reduces to

$$\Gamma_{ij} = \phi_{ai}\phi_{bj}\sum_{n=1}^{N_\omega} \mathrm{Re}(\overline{D_i(\omega_n)} D_j(\omega_n)[S_{ff}(\omega_n)]_{ab})\frac{\Delta\omega}{\pi}. \tag{15}$$

To obtain results at every node, Γ may be evaluated only once while T and the modal sums must be computed at each node. In practice, modal truncation must be

performed; only that part of Γ corresponding to the first M modes is computed where M is sufficiently large to capture the dynamic properties of the structure over the frequency range of interest. Computation of Γ is of order $N_F N_\omega$. Within a modal survey, the total computation is of order $M^2 N$, where N is the number of nodes in the survey. Even for a very large model, these computations are easily accomplished on a workstation. It is anticipated that further economies can be obtained by a formulation that exploits mode acceleration.

5. RESULTS AND VERIFICATION

The shell elements used to model the cylinder in Figure 1 produce no out-of-plane stresses [12]. Therefore, in element co-ordinates, the three remaining non-zero stress components are σ_x, σ_y (normal stress) and τ_{xy} (shear stress). In this context, A reduces to a 3×3 matrix,

$$A = \begin{bmatrix} 1 & -\frac{1}{2} & \\ -\frac{1}{2} & 1 & \\ & & 3 \end{bmatrix}. \tag{16}$$

The transfer functions for the stress components were computed from equation (12) at each grid point in the model. A typical input PSD for transverse excitation of the cylinder is provided in Figure 2 and a typical set of transfer functions at one of the grid points is illustrated in Figure 3. The stress and displacement eigenvectors, Ψ and φ, required to compute the transfer functions were obtained using MSC/NASTRAN, and 1% modal damping was applied.

The mean-squared von Mises stresses at each grid point were calculated using two methods; (1) the method derived above, evaluating equation (5) using the frequency quadrature indicated in equation (15); (2) time realization using equation (1) and an inverse FFT of the stress components constructed in frequency space.

The mean-squared von Mises stresses at each grid point were found to be identical using each of the two methods, thus verifying the procedure.

Time and frequency realizations of the input acceleration and output stresses at a typical point are shown in Figures 4 and 5 respectively. Time and frequency plots for the mean squared and r.m.s. von Mises stresses at the same location are presented in Figure 6. The r.m.s. von Mises stresses at all grid points were computed, with contours of this quantity plotted in Figure 7.

As illustrated in Figure 5, the shear and one of the normal stress components dominate the stress state at this location. σ_y is driven by the first bending mode of the cylinder, at 724 Hz. τ_{xy} is driven by both first and second bending modes, the second occurring at 3464 Hz. The relatively low σ_x stress is driven by all of the first three modes, the third occurring at 7698 Hz.

We see in Figure 6 that the frequency content of the squared von Mises stress contains terms at twice the excited natural frequencies (e.g., 1448 Hz, 6928 Hz). This

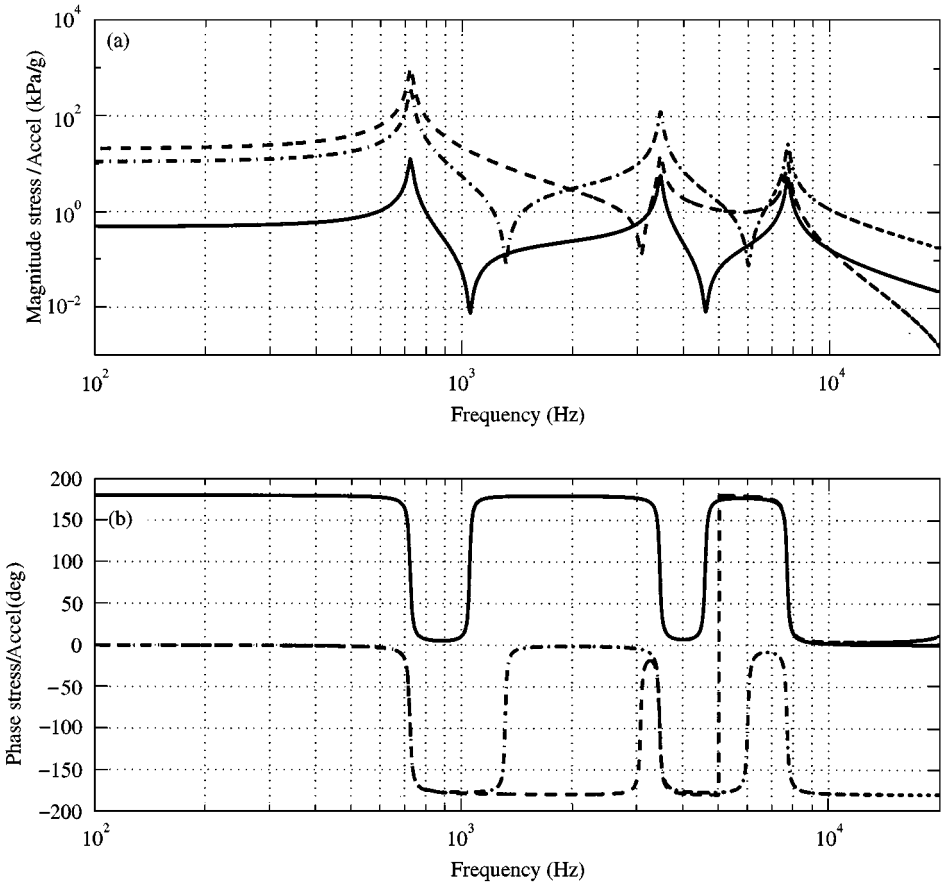

Figure 3. Stress component transfer functions at node 53: (a) magnitude, (b) phase. ——, Normal stress in the x direction; – – –, normal stress in the y direction; – · –, shear stress in the xy plane.

observation is attributable to the fact that a squared sinusoid is another sinusoid at twice the original frequency (plus a DC component). So the linear stress components respond at the natural frequencies of the structure, while the squared von Mises stress responds at these frequencies and at twice these frequencies. At this particular location, the $\sigma_x\sigma_y$ term in the expression for von Mises stress is small and the first two modes, drivers of σ_y and τ_{xy}, also drive the von Mises stress. Note that von Mises stress frequencies also occur at $f_j - f_i$, where i, j denote excited modes. For example, Figure 6 shows von Mises content at $f_2 - f_1 = 3464 - 724 = 2740$ Hz and at $f_3 - f_2 = 7698 - 3464 = 4234$ Hz.

6. COMPARISON WITH MILES' RELATION

Evaluation of r.m.s. von Mises stress using the new procedure and the traditional Miles' relation were compared to identify scenarios in which Miles' relation is inappropriate. A new input acceleration PSD was generated, as shown in Figure 8.

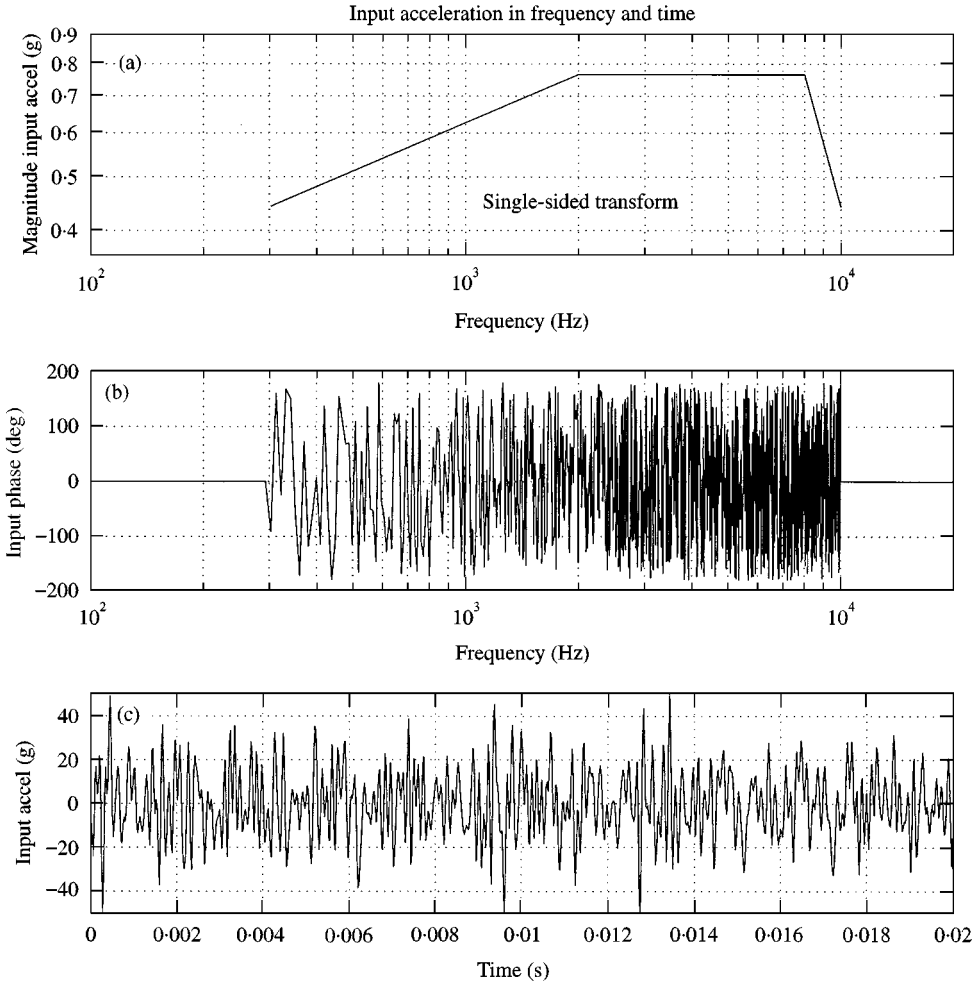

Figure 4. Time and frequency realizations of the lateral input acceleration: (a) magnitude of Fourier transform of input acceleration, (b) phase of Fourier transform of input acceleration, (c) input acceleration in time domain.

Three cases were examined in which the input PSD frequency range was selected to excite (1) only the first mode, (2) only the second mode, and (3) both first and second modes. To excite the first mode only, the input PSD followed the definition of Figure 8 up to 1000 Hz, and was set to zero beyond this frequency. To allow the second mode to dominate, the input PSD was set at zero below 1000 Hz and followed Figure 8 definition between 1000 and 10 000 Hz. Both modes were excited when the full PSD from 0 to 10 000 Hz was applied. A comparison of the exact method for these three cases is discussed below and summarized in Table 1.

Miles' method assumes single-degree-of-freedom behavior of a structure. An additional constraint on the application of Miles' relation to elastic structures is that the shape of the single excited mode must approximate the profile of the structure under a static g-field. For example, the first mode of a cantilever beam

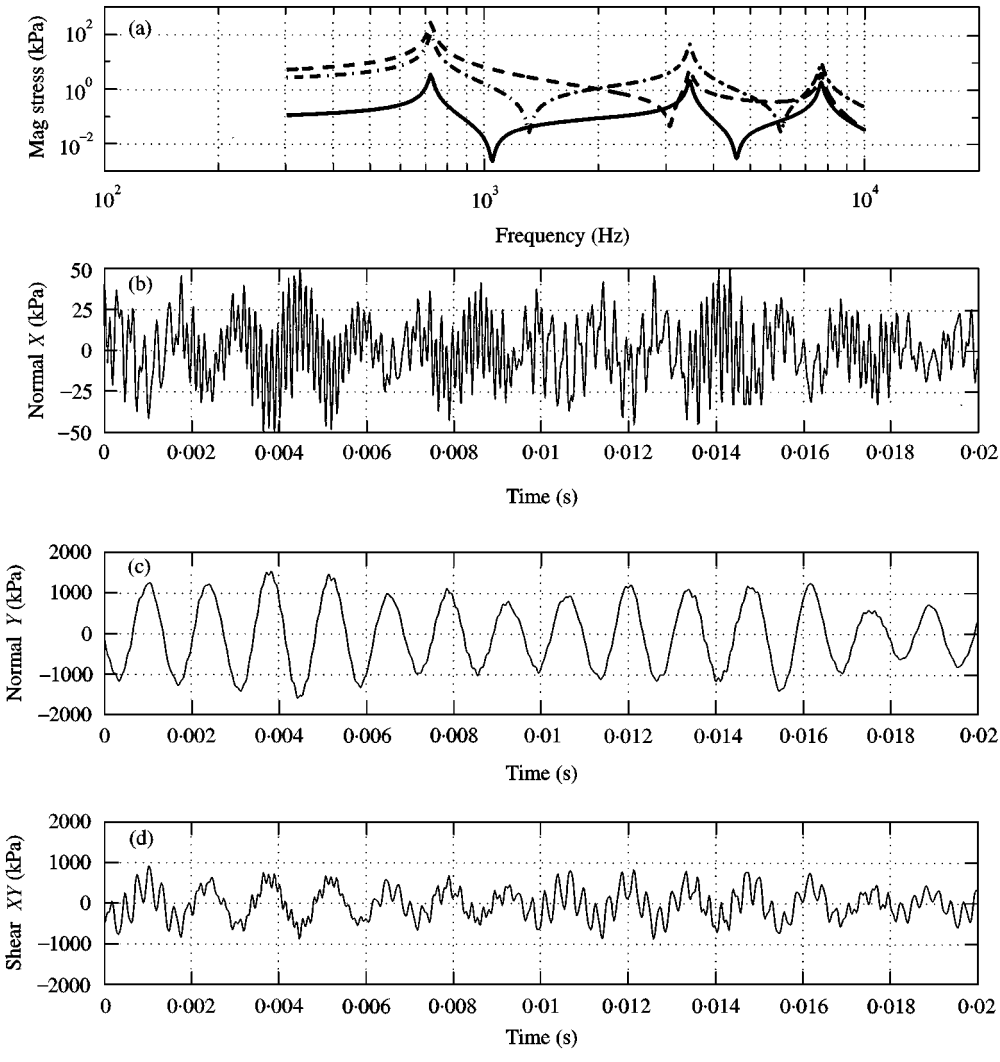

Figure 5. Time and frequency realizations of the output stresses at node 53. (a) Magnitude of Fourier transforms of output stress components (——, normal stress in the x direction; – – –, normal stress in the y direction; – – –, shear stress in the xy plane). (b) Normal component of stress in the x direction in time domain, (c) normal component of stress in the y direction in time domain, (d) shear stress in the xy plane in the time domain.

assumes the approximate shape of the beam under a transverse g-field. Such alignment of vibrational and static models is often not the case.

Miles' relation is given by

$$g_{eq} = \tfrac{1}{2}\sqrt{\omega_m PSD(\omega_n) Q_m}. \tag{17}$$

where g_{eq} is the approximate r.m.s. acceleration response, commonly used as an "equivalent static-g-field", ω_m is the single natural frequency chosen for application of Miles' relation, $PSD(\omega_m)$ is the value of the input acceleration PSD at frequency

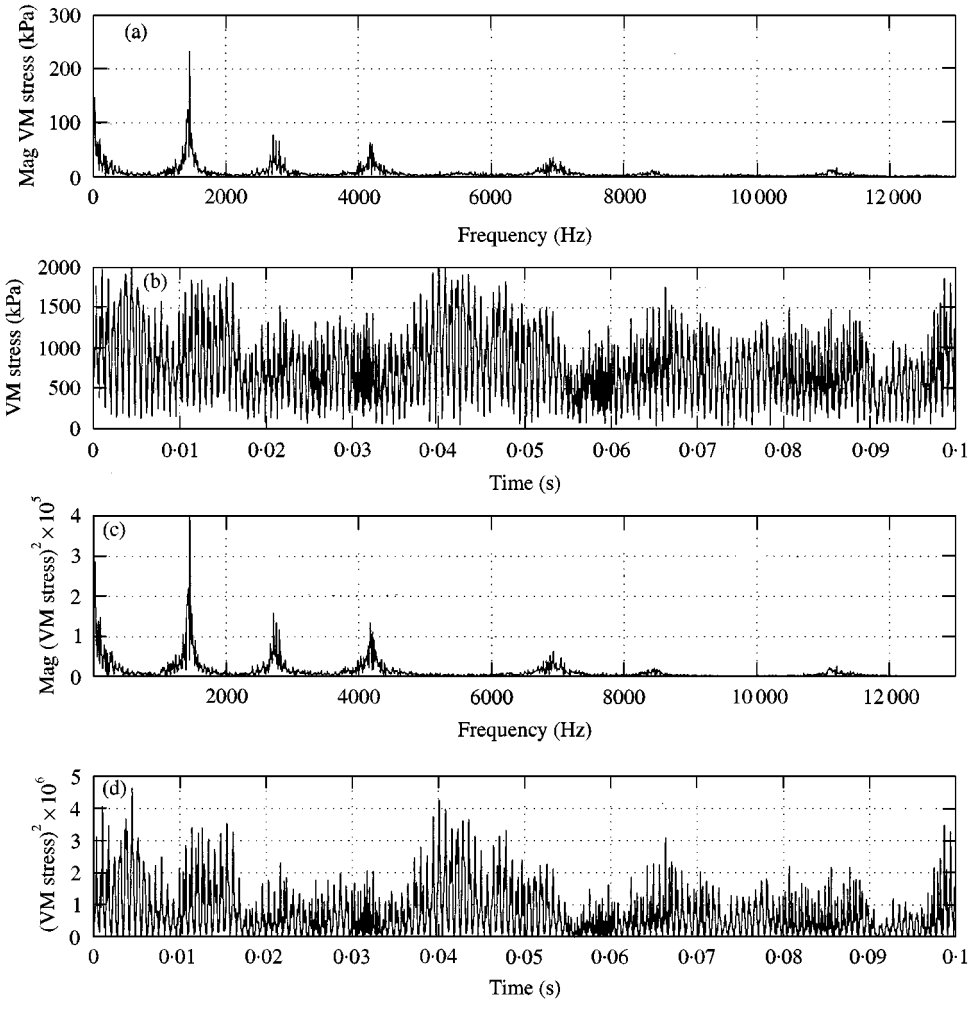

Figure 6. von Mises and squared von Mises stresses at node 53: (a) magnitude of the Fourier transform of von Mises stress, (b) von Mises stress in the time domain (r.m.s. = 868·7 kPa), (c) magnitude of the Fourier transform of the square of von Mises stress, (d) the square of the von Mises stress in the time domain (mean = 754, 993 $(\text{kPa})^2$).

ω_m, and Q_m is the quality factor, defined as $1/(2\gamma_m)$ for the mode. For the input PSD shown in Figure 8, g_{eq} from equation (17) is $10{\cdot}7g$ for the first modal frequency (724 Hz), and $90{\cdot}3g$ for the second modal frequency (3464 Hz).

Because of the von Mises stress in a static g-field scales with the magnitude of the field, the static response of the cantilevered cylinder to a 1-g-field may be used to scale the Miles' approximations for each mode. The displacement and von Mises stress responses to a transverse 1-g-field are presented in Figure 9. The profile of the static response is similar to the first mode of a cantilever beam. The maximum von Mises stress corresponding to the 1-g static field is 86·9 kPa (12·6 psi), and occurs at the base top and bottom-most fibres. Thus, the maximum von Mises stresses

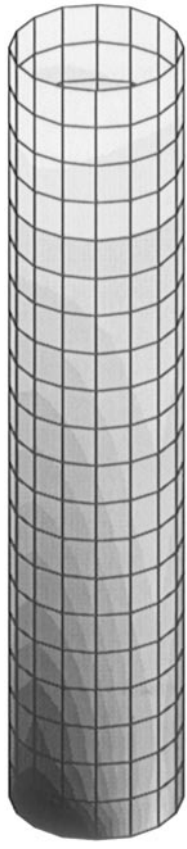

Figure 7. r.m.s. von Mises stress contours.

corresponding to the Miles' equivalents for the first and second modal frequencies are 926·7 kPa (134·4 psi) and 7848·3 kPa (1138·3 psi) respectively. Note that where more than one modal frequency is contained in the input spectrum, Miles' relation becomes ambiguous and probably should not be used.

A comparison of exact values (the method developed in this monograph) with Miles' estimates for r.m.s. von Mises stress for the three input spectra indicated in Figure 8, shows that Miles' method can be conservative or non-conservative, depending on the applied load spectrum.

The true r.m.s. von Mises stresses were computed using the new method presented above. The stress contours which result from the application of the input PSD below 1000 Hz are superimposed upon the deformed shape for the first mode in Figure 10. The stress contours and shape profile closely resemble those of the static-g response. The maximum r.m.s. von Mises stress for this case is 809·4 kPa (117·4 psi), showing Mile's method to be slightly conservative.

When the second mode alone is excited by applying the input PSD above 1000 Hz, an entirely, different result is obtained. The von Mises stress contours for this case are superimposed upon the deformed shape for the second mode in Figure 11.

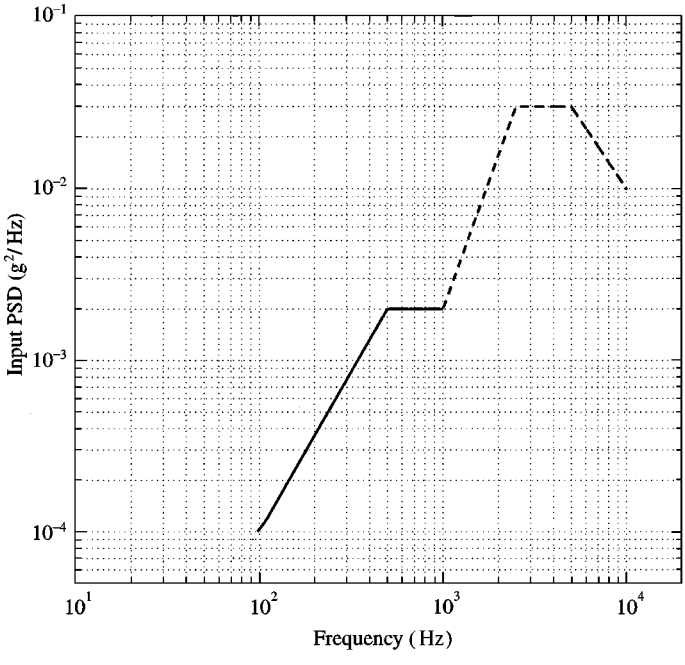

Figure 8. Input acceleration PSD for comparison with Miles' method: ——, portion of PSD used for first mode excitation; – – –, portion of PSD used for second mode excitation.

TABLE 1

Comparison of exact r.m.s. von Mises stress to Miles' approximation for example structure

Spectrum	Exact	Miles' relation
PSD 1(see Figure 8)	809·4 kPa	926·7 kPa
PSD 2 (see Figure 8)	732·9 kPa	7848·3 kPa
Combined PSD	1092·1 kPa	926·7 kPa/ 7848·3 kPa

The stress contours and shape profile do not resemble those of the static-*g* response. The maximum r.m.s. von Mises stress for this case is 732·9 kPa (106·3 psi), showing Miles' method to be conservative by an order of magnitude.

Finally, the entire PSD of Figure 8 was applied to the cylinder, and the resulting von Mises stress contours are superimposed upon the first and second mode shapes in Figures 12 and 13. The contours are observed to be a blend of the two narrow-band responses, with the maximum r.m.s von Mises stress at 1092·1 kPa

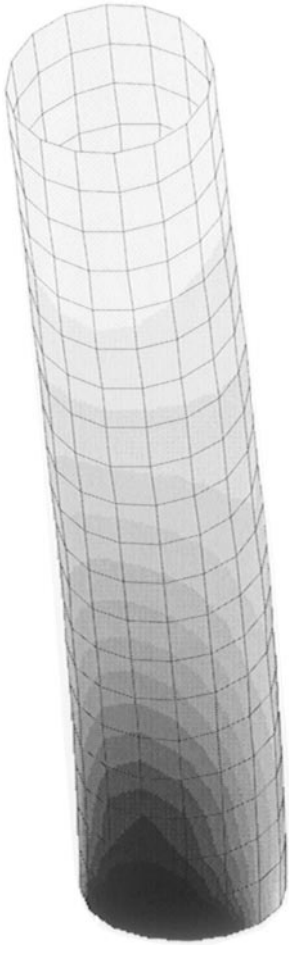

Figure 9. von Mises stress contours and displacements for a transverse 1-g-field.

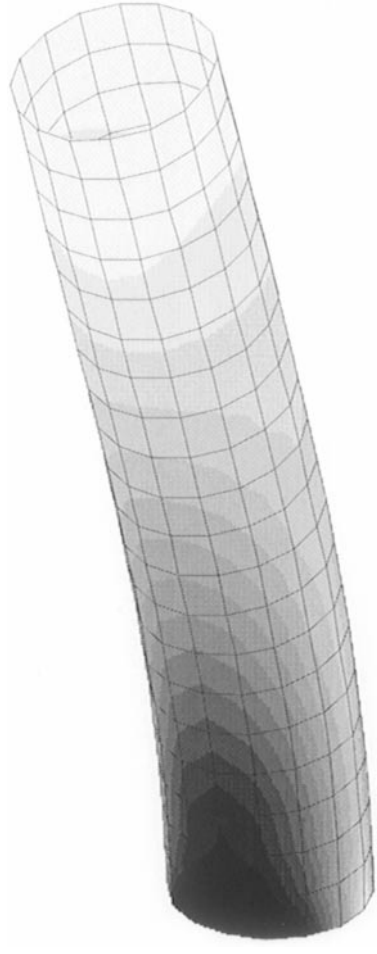

Figure 10. von Mises stress contours for $f_{psd} < 1000$ Hz superimposed upon mode shape 1.

(158·4 psi). The first-mode Miles' approximation is slightly non-conservative, whereas the second-mode approximation is much too conservative.

7. CONCLUSIONS

A computationally efficient method has been developed for calculating the r.m.s. von Mises stress in a random vibration environment. The method retains the full accuracy of the FEM model and modal analysis. Surveys of the r.m.s. stress for the entire structure can be computed efficiently. The number of operations per node output is of order M^2, where M is the number of modes computed. Results exactly match a full-time history development.

Conditions under which Miles' relation produces good estimates of von Mises stress contours were examined, as well as conditions resulting in poor estimates.

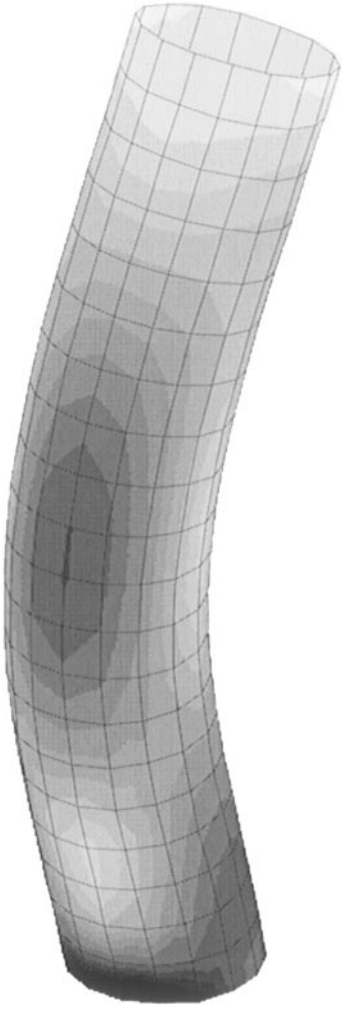

Figure 11. von Mises stress contours for $f_{psd} > 1000$ Hz superimposed upon mode shape 2.

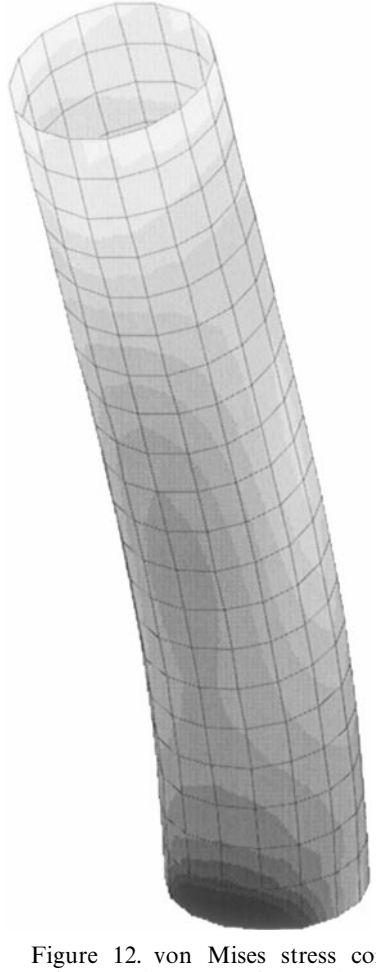

Figure 12. von Mises stress contours for $0 < f_{psd} < 10$ kHz superimposed upon mode shape 1.

Miles' relation is adequate when the system response is dominated by a single mode, and when the excited mode shape approximates the response to a static g-field. Otherwise, both conservative and non-conservative estimates may result from the application of Miles' relation.

The exact method presented here is quite efficient; it can be used to make contour plots of von Mises stress corresponding to anticipated input force spectra for each of several candidate designs. This process should facilitate the systematic use of random vibration criteria in the design process. Work underway will further quantify the statistical properties of the von Mises stress.

Finally, the methods presented here could be applied equally well to any other symmetric, quadratic function of the structural response.

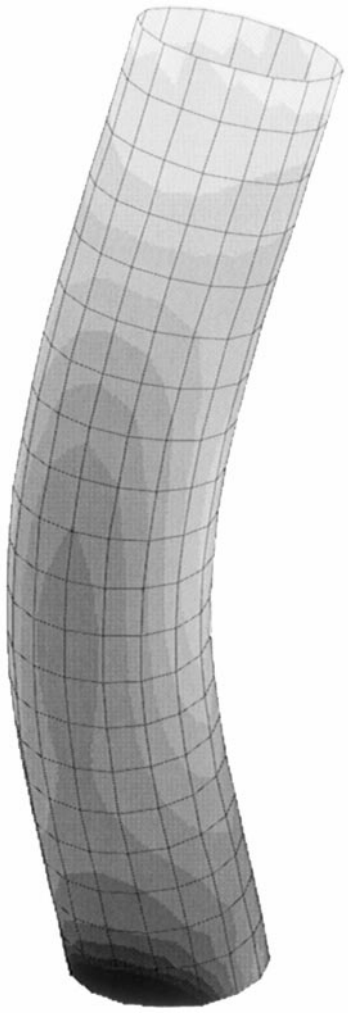

Figure 13. von Mises stress contours for $0 < f_{psd} < 10\,\text{kHz}$ superimposed upon mode shape 2.

ACKNOWLEDGMENT

Sandia National Laboratories is a multiprogram laboratory operated by Sandia Corporation, a Lockheed Martin Company, for the United States Department of Energy under Contract DE-ACO4-94AL85000.

REFERENCES

1. A. H. Jazwinski 1970 *Stochastic Processes and Filtering Theory*. New York: Academic Press.
2. Y. K. Lin 1967 *Probabilistic Theory of Structural Dynamics*. Malabar, FL: Robert E. Krieger Publishing Co.
3. P. H. Wirshing, T. L. Paez and K. Ortiz 1995 *Random Vibrations*. New York: John Wiley & Sons.

4. J. W. MILES 1954 *Journal of the Aeronautical Sciences* **21**, 753–762. On structural fatigue under random loading.
5. R. C. FEREBEE and J. H. JONES 1984 *NASA/Marshall Space Flight Center Report*, ID: 19910073736N (91N71291). Comparison of Miles' relationship to the true mean square value of response for a single degree of freedom system.
6. D. C. KAMMER, C. C. FLANIGAN and W. DREYER 1986 *Proceedings of the 4th International Modal Analysis Conference*. A superelement approach to test-analysis model development.
7. L. E. MALVERN 1969 *Introduction to the Mechanics of a Continuous Medium*. Englewood Cliffs, NJ: Prentice-Hall.
8. L. MEIROVITCH 1975 *Elements of Vibration Analysis*. New York: McGraw-Hill.
9. W. RUDIN 1966 *Real and Complex Analysis*. New York: McGraw-Hill.
10. J. BENDAT and A. PIERSOL 1986 *Random Data: Analysis and Measurement Procedures*. New York: John Wiley & Sons.
11. H. MADSEN 1985 *Journal of Engineering Mechanics* **111**, 1121–1129. Extreme-value statistics for nonlinear stress combination.
12. K. KILROY (editor) 1998 *MSC/NASTRAN Quick Reference Guide, Version* 70.5. Los Angeles: MacNeal-Schwendler Corp.
13. R. R. CRAIG Jr 1981 *Structural Dynamics, An Introduction to Computer Methods*. New York: John Wiley & Sons.

APPENDIX A: CALCULATION OF Q WHERE INPUT FORCES ARE NOT ALL ZERO MEAN

The evaluation of the zero time-lag covariance matrix presented in the body of this monograph assumed that the applied loads were each of zero mean. This limitation was introduced in order to use frequency domain techniques that are otherwise not convergent. This restriction on the input loads is removed by the following decomposition of the problem.

We consider random loads applied to the structure assuming that they are stationary but not zero mean. Similarly, the stationary modal response will also not have zero mean. The vector of modal co-ordinates, q, is decomposed as

$$q = \bar{q} + \delta q, \tag{A.1}$$

where $\bar{q} = E[q]$. Note that δq does have zero mean. Substituting equation (A.1) into equation (7) and then into equation (5) we have

$$E[p^2(t)] = \sum_{i,j}^{M} \Gamma^0_{ij} T_{ij} + \sum_{i,j}^{M} \Gamma^1_{ij} T_{ij}, \tag{A.2}$$

where

$$\Gamma^0_{ij} = \bar{q}_i \bar{q}_j, \qquad \Gamma^1_{ij} = E[\delta q_i(t)\, \delta q_j(t)]. \tag{A.3, A.4}$$

Calculation of Γ^0 is performed below. Calculation of Γ^1 is performed exactly as is done in the body of this monograph.

The vectors $\bar{q}$ are static solutions of the linear structure:

$$\bar{q} = \Omega^{-2} \varphi^{\mathrm{T}} \bar{f}. \tag{A.5}$$

where φ is the matrix whose columns are the mass-normalized eigenvectors of the system. Ω is the diagonal matrix whose elements are the natural frequencies of the corresponding column of φ, f is column vector of applied loads, and $\bar{f} = E[f]$. The matrix Γ^0 is evaluated easily from equations (A.3) and (A.5). In evaluating equation (A.5), terms in Ω^{-2} associated with rigid-body modes are set to zero to avoid a devide-by-zero error. This is permissible, since the corresponding modal stresses are zero.

APPENDIX B: NOMENCLATURE

$f(t)$	column vector of all load components on the structure at time t
$\hat{f}$	frequency domain representation of load vector $f(t)$
$p(t)$	von Mises stress at time t
$D_j(\omega)$	frequency dependence in modal transfer functions
H	transfer function matrix
N_ω	number of quadrature points in numerical integration over frequency space
N_F	number of input force locations
PSD	power spectral density of input forces
r.m.s.	root-mean-square
S_{ff}	input force cross-spectral density matrix
$R_{xy}(\tau)$	matrix of covariances of the Cartesian product of column vectors x and y
$\sigma(t)$	stress vector (6×1)
$q_k(t)$	kth modal co-ordinate
φ_{ai}	displacement eigenvector for mode i at degrees of freedom a
Ψ_i^σ	stress vector for mode i
$(\ )^{\mathrm{T}}$	matrix transpose
$E[\ ]$	expected value operator
$\bar{(\ )}$	complex conjugate
$(\ )^\dagger$	Hermitian (complex conjugate transpose)
γ_k	modal damping factor for kth mode